arXiv:1510.00885v2 [physics.atom-ph] 28 Nov 2015

# Polarization measurement of Cs using the pump laser beam

Jiancheng Fang, Rujie Li,* Lihong Duan, Wenfeng Fan, and Liwei Jiang
*School of Instrument Science and Opto-electronics Engineering, Beihang University, Beijing 100191, China*
*Science and Technology on Inertial Laboratory, Beihang University, Beijing 100191, China*
(Dated: December 1, 2015)

In the optical pumping systems based on the pump-probe arrangement, the spin polarization of the atoms is generally monitored utilizing the probe laser beam, in which way an extra perturbation must be introduced and thus affects the normal operation of the sensors. By investigating the absorption rate of the circularly polarized pump laser, here we demonstrate the feasibility of extracting the electron-spin polarization from the transmitted pump laser intensity. We experimentally validate the method in a spin-exchange relaxation free (SERF) magnetometer and the results are in excellent agreement with the theory. The scheme operates in a non-perturbative mode and features a real-time observation. We also study the corresponding magnetic field response of the SERF magnetometer and a term arising from the diffusion effects has been added to the original model to explain the discrepancy of the response.

PACS numbers: 32.10.Dk, 32.80.Xx, 07.55.Ge, 42.25.Bs

## I. INTRODUCTION

In optical pumping, absorption of the near-resonance circularly polarized light could lead to large population imbalances in atomic ground states and induce the polarization of the atoms [1]. A variety of applications, from traditional studies on nuclear resonance gyroscope [2], atomic clock [3, 4], optical pumped magnetometer [5–7] to the recently developed experiments in atomic spin gyroscope [8, 9], have use the electron-spin polarization for precise measurements. Among them, the recently developed SERF magnetometer features a higher sensitivity and a much more portable package, compared to the superconducting quantum interference devices (SQUIDs), thus provides a better way to measure magnetocardiography (MCG) and magnetoencephalography (MEG) signals [10, 11]. With a sufficient high cell temperature and weakly shielded environment, such that $1/T_{se} \gg \omega_0$ ( $T_{se}$ is the time between spin-exchange collisions and $\omega_0$ is the spin precession rate), the spin-exchange collisions would not broaden the magnetic resonance linewidth and it indicates the realization of the SERF regime [5]. As the operation principle of the sensors mentioned above relies on the spin polarization, the value of the polarization would affect the performance of these sensors. Thus, it is necessary to monitor the polarization of the alkali-metal atoms. A general experimental technique by turning the pump laser beam on and off has been used to calculate the spin polarization [12]. By applying an oscillating magnetic field, the transverse electronic paramagnetic resonance (EPR) spectroscopy is another efficient method to obtain the population status [13, 14]. However, both of these processes would introduce an extra perturbation into the sensor proper and affect its normal operation.

The motivation of this article is to develop a non-perturbative scheme to acquire the polarization of the electron-spin while minimizing the introduction of perturbation to the system. By investigating the relationship between the electron-spin polarization and the transmission of the circularly polarized pump laser beam, here we propose a new scheme, which only relies on the pump laser intensity, to extract the electron-spin polarization. Compared to the previous methods, this technique has the advantage that no extra disturbance is introduced into the sensor. Besides, this scheme could achieve a real-time observation and requires less components. We experimentally validate the method in a SERF magnetometer and the results are in excellent agrement with the theory. The model could deep our understanding of the absorption process of the pump laser and facilitate the optimization of the polarization in the atomic sensors.

## II. THEORETICAL MODEL

The electron-spin polarization of the alkali-metal atoms along the $z$ direction (pumping axis) $P_z^e$ is defined by [15]

$$P_z^e = \frac{R_{op}}{R_{op} + R_{sd}} \tag{1}$$

where $R_{op}$ is the optical pumping rate due to the circularly polarized pump laser, $R_{sd}$ is the spin-destruction rate due to collisions with other alkali atoms, buffer gas atoms and quenching gas molecules [16]. While the atoms illuminated by the pump laser are polarized, those atoms outside the illumination region still could be polarized by the diffusion effects. And the diffusion length in one relaxation time is $z_d = \sqrt{D/R_{sd}}$, where $D$ is the diffusion coefficient [17]. Under typical experimental condition of the Cs magnetometer, where $R_{sd} \approx 300$ 1/s and $D = 39$ mm$^2$/s, the corresponding diffusion length is about 0.36

* lirujie@buaa.edu.cn

mm [16]. For a monochromatic laser, the optical pumping rate could be described by

$$R_{op} = kI(z) \tag{2}$$

where $k$ determined by the photo absorption cross-section as well as the waist of the laser beam is defined as the pumping rate per unit laser intensity [12, 13], $z$ is the position in the cell and $I(z)$ is the corresponding laser intensity. Inserting Eq. (2) into Eq. (1), we arrive at the following expression for the spin polarizatioin as a function of the pump laser beam:

$$P_z^e = \frac{I(z)}{I(z) + 1/K} \tag{3}$$

where the coefficient $K$ is defined as $K = k/R_{sd}$. Note that Eq. (3) gives us the relationship between the electron-spin polarization and the laser intensity. If the value of $K$ is known, then Eq. (3) provides a useful method to measure the atomic spin polarization.

As the pump beam with circular polarization propagates through the vapor cell, the the populations of the atoms are redistributed and the reduction in the laser intensity $I(z)$ is given by [18]

$$\frac{\mathrm{d}I(z)}{\mathrm{d}z} = -n\sigma(\nu) I(z) (1 - P_z^e) \tag{4}$$

where $n$ is the density of the alkali vapor, $\sigma(\nu)$ is the absorption cross-section determined by the atomic frequency response about the resonance frequency $\nu$. Eq. (4) could be solved via the Lambert $W$-function [19], and the solution is expressed as

$$I(z) = \frac{R_{sd}}{k} W\left(\frac{kI(0)}{R_{sd}} \exp\left(\frac{kI(0)}{R_{sd}} - n\sigma(\nu)z\right)\right) \tag{5}$$

where $W(z)$ satisfies the function $W(z)e^{W(z)} = z$, $I(0)$ and $kI(0)$ represent the incident laser intensity and the corresponding pumping rate.

To facilitate the data fitting, we rewrite Eq. (5) in a much more simplified form,

$$I(z) = \frac{1}{K} W\left(KI(0) \exp\left(KI(0) - O\right)\right) \tag{6}$$

where $k/R_{sd}$ is replaced by $K$ and $O = n\sigma(v)l$ is the optical depth of the cell. The transmitted laser intensity, $I(z)$, the incident laser intensity, $I(0)$, could be measured directly. The value of $K$ as well as the optical depth of the cell, $O$, are the free parameters and could be obtained from the fit based on Eq. (6).

Substituting the values of $K$ and the transmitted pump beam intensity $I(z)$, which could be monitored continuously, into Eq. (3), we would obtain the corresponding electron-spin polarization in real time. Note that Eqs. (3) and (6) only rely on the intensity of the pump laser, which is the essential part of the devices mentioned above, thus this scheme could be conducted without adding any additional component. Meanwhile, no perturbation has been introduced into the sensor proper.

A magnetic field $B_y$, which is applied perpendicular to the magnetic moment arising from the polarized atoms, will cause a torque on the atom and induce the Larmor precession of the atom. The precession of the spin polarization $P_z^e$ will result in a projection of on the $x$ axis, indicated as $P_x^e$. For the ultra-sensitive SERF magnetometry, the component $P_x^e$ is generally detected by a linear polarized probe beam and the magnetic field response could be expressed as [18],

$$P_x^e \approx \frac{P_z^e \gamma_e}{R_{op} + R_{sd}} B_y \tag{7}$$

where $P_x^e$ is the $x$ projection of the spin polarization $P_z^e$ and $\gamma_e = g_s\mu_B/\hbar$ is the gyromagnetic ratio of a bare electron. $P_x^e$ could be detected via the optical rotation of a linearly polarized probe beam, given by [20]

$$\theta(\nu) = \frac{\pi}{2} l n r_e c f P_x^e \sum_{F_g,F_e} B_{F_g,F_e} \mathrm{Im}\left[V\left(\nu - \nu_{F_g,F_e}\right)\right] \tag{8}$$

where $l$ is the path length of the probe beam through the cell, $r_e = e/(m_e c^2) = 2.818 \times 10^{-15}$ m is the classical electron radius ($e$ and $m_e$ are the electric charge and the mass of the electron), $c$ is the speed of the light, $f$ is the oscillation strength (roughly 1/3 for $D1$ transition and 2/3 for $D2$ transition), $V\left(\nu - \nu_{F_g,F_e}\right)$ is optical resonance lineshape of the probe beam with Voigt profile, $\nu$ is the frequency of the probe light and $\nu_{F_g,F_e}$ is the resonance frequency of the transition $F_g \to F_e$, $B_{F_g,F_e}$ is the strength of the optical rotation arising from the individual hyperfine resonance $F_g \to F_e$ and $\sum B_{F_g,F_e} = 1$. A step in the $B_y$ field with an amplitude of 0.05 nT has been applied at each pump laser intensity and the response should be maximized when the spin polarization is equal to 50% according to Eq. (7).

## III. EXPERIMENT DETAILS

The configuration of the experimental setup used is depicted in Fig. 1, and is centered around a spherical vapor cell with a diameter of 12 mm. The vapor cell contains a droplet of Cs metal, 50 Torr of $N_2$ gas and 500 Torr of $^4$He gas. The $N_2$ prevents radiation trapping, while $^4$He was included to reduce the diffusion effect to the cell walls. It was held in an oven heated to 100 °C with twisted-pair wires driven by AC current at 50 kHz. A set of four cylindrical layers of $\mu$-metal magnetic shield enclosed the cell and provides a shielding factor of $10^6$ to quasi-static magnetic fields. The vapor cell was optically pumped by a circularly polarized pump beam originating from a distributed feedback (DFB) laser. The pump laser, with a spectral width of about 2 MHz, was tuned to the Cs $D_1$ resonance line and directed along the $z$ axis. According to Eq. (5), the transmitted laser intensity $I(z)$ would vary with the different incident laser intensity. The incident and the transmitted laser intensities were recorded by two photodiodes (PD1 and PD2), simultaneously.

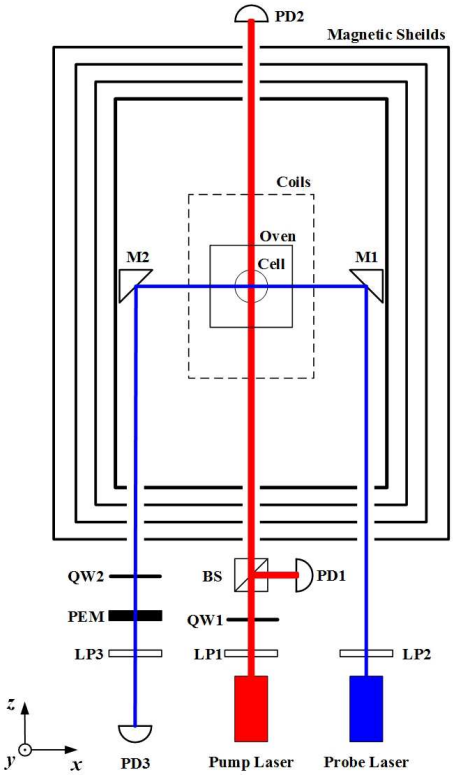


FIG. 1. Experimental setup. LP1, LP2 and LP3: linear polarizer, QW1 and QW2: quarter waveplate, BS: beam splitter, M1 and M2: reflection mirror, PD1, PD2 and PD3: silicon photodiodes, PEM: photo-elastic modulator. Red lines mark the pump laser path, while blue lines indicate the probe laser path.

The probe laser beam, formed by another DFB system, is detuned by about 0.3 nm to the red side of the $D_2$ resonance line and propagates in the $x$ axis. The first calcite polarizer (LP2) determines the initial linear polarization axis at 0°. Faraday rotation from the atoms rotates the polarization plane of the probe beam by an angle $\theta$ according to Eq. (8). Then, a quarter waveplate (QW2) with one of its axes nominally aligned with the calcite polarizer contributes a circular component proportional to $\theta$. A final calcite polarizer (LP3), which acts as an analyzer and is crossed with the original polarizer, selects the time varying intensity of the transmitted light. A photo-elastic modulator (PEM) following the quarter waveplate is used to modulate the polarization of probe laser in order to improve the S/N (the ratio of signal to noise). And the modulation axis of the PEM is oriented at 45° with respect to the transmission axis of the polarizer. Finally, the probe beam transmitted through the cell is detected by a photodiode (PD3) and the time-varying intensity on PD3 is given by [15]

$$I^{\mathrm{p}}(t) \approx I_0^{\mathrm{p}} \alpha\theta \sin(\omega t) \tag{9}$$

where $I_0^{\mathrm{p}}$ is the incident intensity of the probe beam, $\alpha \approx 0.08$ rad and $\omega \approx 50$ $k$Hz are the depth and the frequency of the PEM modulation. Note that the time-varying intensity of the probe beam $I^{\mathrm{p}}(t)$ is definitely different from the distance-dependent intensity of the pump beam $I(z)$. The photocurrent is amplified by a low-noise transimpedance amplifier and demodulated by a commercial computer-controlled digital lock-in amplifier (Zurich Instruments, model HF2LI) referenced to the PEM. Via detecting the optical rotation of the polarization plane, the residual magnetic fields could be further canceled actively by three orthogonal coils inside the shields in order to realize the SERF regime [21]. Under the SERF regime, the spin relaxation arising from the spin-exchange collisions is completely eliminated and the spin-destruction collisions dominate the absorption of the pump laser.

## IV. RESULTS AND DISCUSSIONS

In Fig. 2, we plot the transmitted laser intensity as a function of the incident laser intensity at room temperature and 100 °C. The density of the vapor cell at room temperature ($n \approx 5.0 \times 10^{10}\mathrm{cm}^{-3}$) is more than two orders less than that at 100 °C ($n \approx 1.6 \times 10^{13}\mathrm{cm}^{-3}$), and the absorption due to the atoms at room temperature is ignorable. As the blue triangles shown in Fig. 2, the transmitted laser intensity is proportional to the incident laser intensity and the reduction of the laser intensity

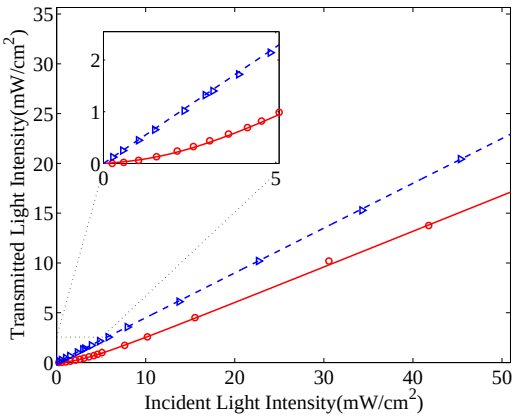


FIG. 2. The transmitted laser intensity as a function of the incident laser intensity of the circularly polarized pump beam. The blue triangles indicate the transmission of pump beam at the room temperature while the blue dashed line is the corresponding linear fitting curve. The red circles are obtained at 100 °C and the red line overlapping the data points is the fitting curve according to Eq. (6), from which the value of $K$ is deduced. The inset shows magnification of the transmission curves. Note that the linearly polarized components of the pump laser beam would be completely absorbed by the hot atoms and thus contribute to the further reduction of the pump laser intensity. In our experiment, the degree of the pump beam polarization is approximately 0.9 and this factor should be included in the curve fitting process based on Eq. (6).

reflects the transmission of the system components, including the uncoated optical glass windows, focus lenses as well as the vapor cell made from aluminosilicate glass. Compared to the results obtained at room temperature, the data points at 100 °C show nonlinear absorption when the incident intensity is less than about 1 mW (see inset in Fig. 2), in which the value of $K$ could be extracted form the fitting according to Eq. (6). However, at high laser intensity the transmitted laser intensity $I(z)$ scales linearly with $I(0)$, which implies that the atoms are almost fully polarized.

Utilizing the coefficient $K$ obtained above and the incident laser intensity, we could achieve the polarization measurements of the electron-spin using Eq. (3). The electron-spin polarization of Cs atoms as a function of the incident laser intensity is shown in Fig. 3. The measured values based on Eq. (3) agree very well with the prediction described by Eq. (1).

The dependence of the magnetic response on the electron polarization has also been studied. The magnetometer responses contained in Eq. (9) are extracted by the lock-in amplifier and are shown in Fig. 4.

The magnetometer signal increase with the incident laser intensity in the weak intensity range of $0 \sim 1$ mW and the system achieves the maximum value when the polarization is nearly 50%, shown in Fig. 4. However, the values at hight intensity deviate from the theory, which we suspect it is the result of the diffusion effects and the model described by Eq. (7) need to be modified. The polarization of the atoms outside the illumination region degrades as the distance $x$ from the illumination region increases,

$$P^e_{zd}(x) \approx P^e_z(1 - e^{-x/z_d}) \tag{10}$$

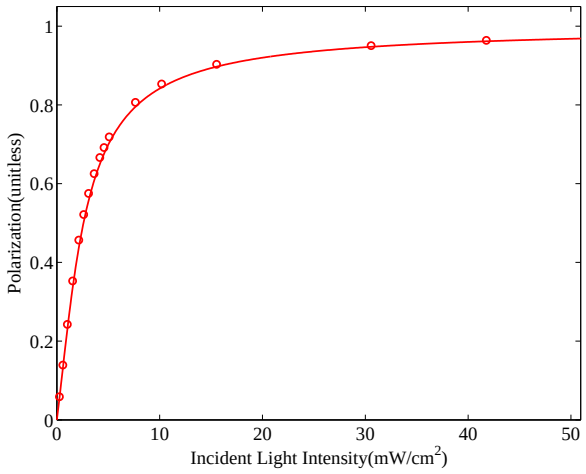


FIG. 3. The polarization of the alkali-metal atoms as a function of the pump beam intensity. The red circles indicate the polarization of the alkali-metals deduced from the intensity of the circularly polarized pump laser based on Eq. (3), while the theoretical prediction according to Eq. (1) is marked by the red line.

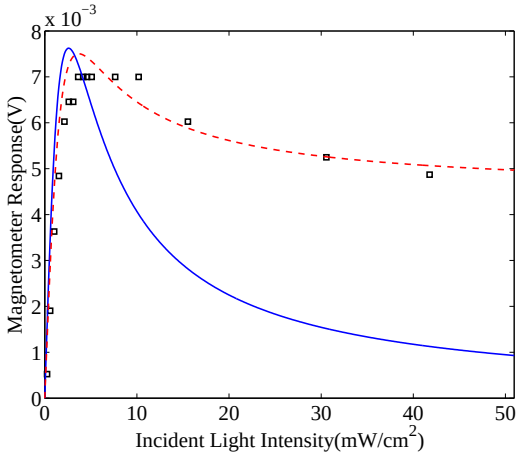


FIG. 4. The magnetometer responses as a function of the pump beam intensity. The black squares indicate the magnetometer response to a step magnetic field along $y$ axis ($\triangle B_y \approx 50$pT) at different pump laser intensity. The blue line shows the unmodified model based on Eq. (8) while the red dashed line is the fitting curve according to the modified version of Eq. (8), where the diffusion term described by Eq. (11) should be included.

where the initial polarization $P^e_{zd}(x \to 0) = P^e_z$. The polarization of the atoms outside the illumination region also contributes to the final response of the magnetic field. To get the corresponding contribution from $P^e_{zd}(x)$ to the rotation signal similar to Eq. (7), we need to know the $x$ projection arising from the polarized atoms in the diffusion region. It could be obtained by integrating $P^e_{zd}(x)$ over the diffusion length, given by

$$P^e_{xd} \approx \frac{P^e_z \gamma^e}{R_{sd}} \frac{z_d}{e} B_y \tag{11}$$

where the term associated with the optical pumping rate has been dropped out compared to Eq. (7). The rotation angle arising from Eq. (11) should be accounted for and added to Eq. (8). As the red dashed line shown in Fig. 4, the fitting curve based on the modified model fit the data better. As the contribution from Eq. (11) depends on the species of the alkali-metal atoms and the noble gases as well as the cell pressure, thus the total optimal polarization would deviate from 50% and tends to become greater. Note that the specific optimal value would not be a constant and changes with the cell parameters of the system.

## V. CONCLUSIONS

In summary, we have studied the relationship between the electron-spin polarization and the intensity of the circularly polarized pump laser, based on which a scheme has been proposed to extract the electron-spin polarization. Compared to the traditional methods to obtain the

polarization, this technique only relying on the transmitted pump laser intensity operates in a non-perturbative mode and has the advantage that no extra disturbance is introduced into the sensor. We therefore anticipate that the scheme described here could detect real-time polarization without disturbing the normal operation of the sensor. A comparison of the experimental results with theoretical calculations is also presented. The experimental results are in excellent agreement with the theoretical prediction and verify the validity of the scheme proposed here. We also investigated the corresponding magnetic field response of the SERF magnetometer as a function of the electron-spin polarization. And a modified model, where we has added the diffusion term to the original model, has been reported to explain the discrepancy of the response between the experimental data and the theory.

As the atomic spin polarization can be derived from the intensity of transmitted pump laser beam, the transmitted intensity could be used to maintain the stability of the pump beam intensity and thus keep the electron spin polarization stable. This strategy allows to reduce the number of components in the pumping systems and results in a simplification of the system structure. From our perspective, our results give new insight into the laser absorption progress for many optical pumping systems, and especially useful for the magnetometer or comagnetometer operated in the SERF regime.

## ACKNOWLEDGMENTS

The authors would like to acknowledge Yao Chen for preparation of the vapor cells. This work is supported by the National Natural Science Foundation of China under Grant No. 61227902.

[1] W. Happer, Rev. Mod. Phys. **44**, 169 (1972).
[2] K. F. Woodman, P. W. Franks, and M. D. Richards, J. Navigation **40**, 366 (1987).
[3] J. Camparo, J. Coffer, and J. Townsend, J. Opt. Soc. Am. B **22**, 521 (2005).
[4] S. Knappe, P. Schwindt, V. Shah, L. Hollberg, J. Kitching, L. Liew, and J. Moreland, Opt. Express **13**, 1249 (2005).
[5] J. C. Allred, R. N. Lyman, T. W. Kornack, and M. V. Romalis, Phys. Rev. Lett. **89**, 130801 (2002).
[6] I. Fescenko, P. Knowles, A. Weis, and E. Breschi, Opt. Express **21**, 15121 (2013).
[7] H. J. Lee, J. H. Shim, H. S. Moon, and K. Kim, " Opt. Express **22**, 19887 (2014).
[8] M. Smiciklas, J. M. Brown, L. W. Cheuk, S. J. Smullin, and M. V. Romalis, Phys. Rev. Lett. **107**, 171604 (2011).
[9] J. Fang, S. Wan, and H. Yuan, Appl. Optics. **52**, 7220 (2013).
[10] K. Kim, S. Begus, H. Xia, S.-K. Lee, V. Jazbinsek, Z. Trontelj, and M. V. Romalis, "Multi-channel atomic magnetometer for magnetoencephalography: A configuration study," Neuroimage **89**, 143-151 (2014).
[11] C. Johnson, P. D. Schwindt, and M. Weisend, Appl. Phys. Lett. **97**, 243703 (2010).
[12] B. Lancor, E. Babcock, R. Wyllie, and T. G. Walker, Phys. Rev. A **82**, 043435 (2010).
[13] S. Appelt, A. Ben-Amar Baranga, C. J. Erickson, M. V. Romalis, A. R. Young, and W. Happer, Phys. Rev. A **58**, 1412 (1998).
[14] A. Ben-Amar Baranga, S. Appelt, C. J. Erickson, A. R. Young, and W. Happer, Phys. Rev. A **58**, 2282 (1998).
[15] S. J. Seltzer, Ph.D Dissertation, Princeton University, 2008.
[16] J. Fang, R. Li, L. Duan, Y. Chen, and W. Quan, Rev. Sci. Instrum. **86**, 073116 (2015).
[17] I. A. Sulai, R. Wyllie, M. Kauer, G. S. Smetana, R. T. Wakai, and T. G. Walker, Opt. Lett. **38**, 974 (2013).
[18] R. Wyllie, Ph.D Dissertation, University of Wisconsin-Madison, 2012.
[19] C. Hwang, and Y.-C. Cheng, Automatica **41**, 1979 (2005).
[20] S. J. Seltzer, and M. V. Romalis, J. Appl. Phys. **106**, 114905 (2009).
[21] J. Fang, and J. Qin, Rev. Sci. Instrum. **83**, 103104 (2012).